Supporting Information

Bimetallic Zeolitic Imidazolate Framework-Derived Iron-, Cobalt- and Nitrogen-Codoped Carbon Nano-Polyhedra Electrocatalyst for Efficient Oxygen Reduction

Zhaowen Hu [a], Zhiyuan Guo [a], Zhengping Zhang [a, b,], Meiling Dou [a, b,]*, Feng Wang [a, b,]*,*

[a] State Key Laboratory of Chemical Resource Engineering, Beijing Key Laboratory of Electrochemical Process and Technology for Materials, Beijing University of Chemical Technology, Beijing 100029, P R China

[b] Beijing Advanced Innovation Center for Soft Matter Science and Engineering, Beijing University of Chemical Technology, Beijing 100029, P. R. China

*Corresponding author: E-mail: wangf@mail.buct.edu.cn (F. Wang); douml@mail.buct.edu.cn (M. L. Dou); zhangzhengping@mail.buct.edu.cn (Z.P. Zhang), Tel. / Fax: 86-10-64451996.

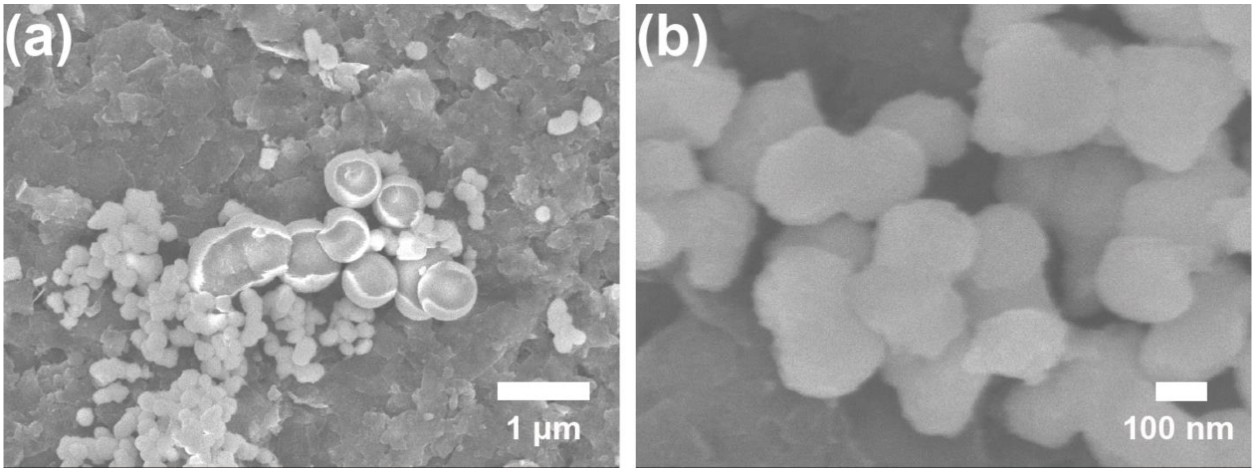

Fig. S1. Low (a) and high (b) magnification SEM images of Fe,Co-ZIF(*0.2*) synthesized under ambient condition

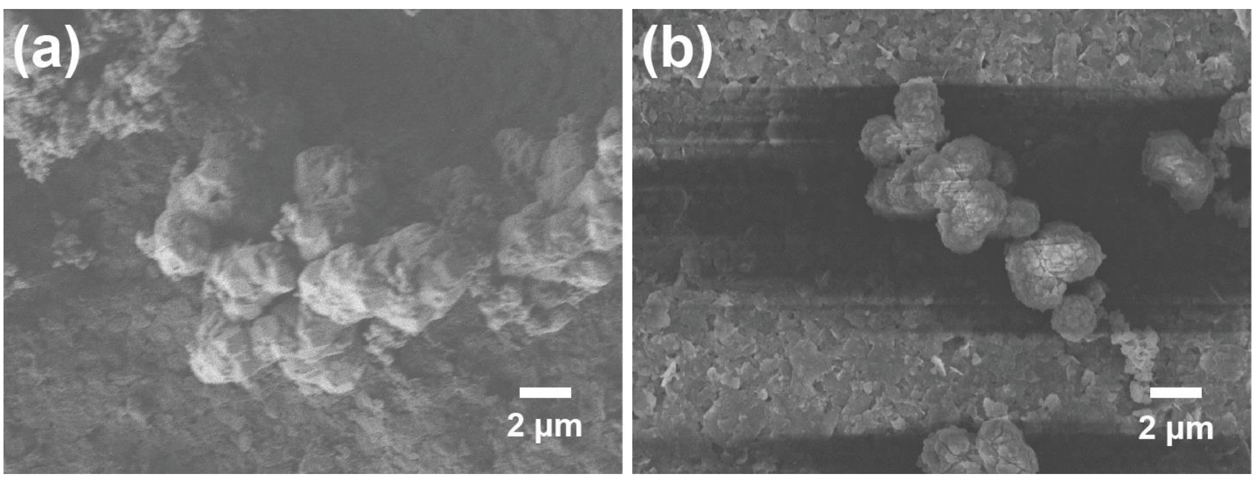

Fig. S2. SEM image of Fe,Co-ZIF with the Fe/Co ratio of 0.5 (a) and 1.0 (b)

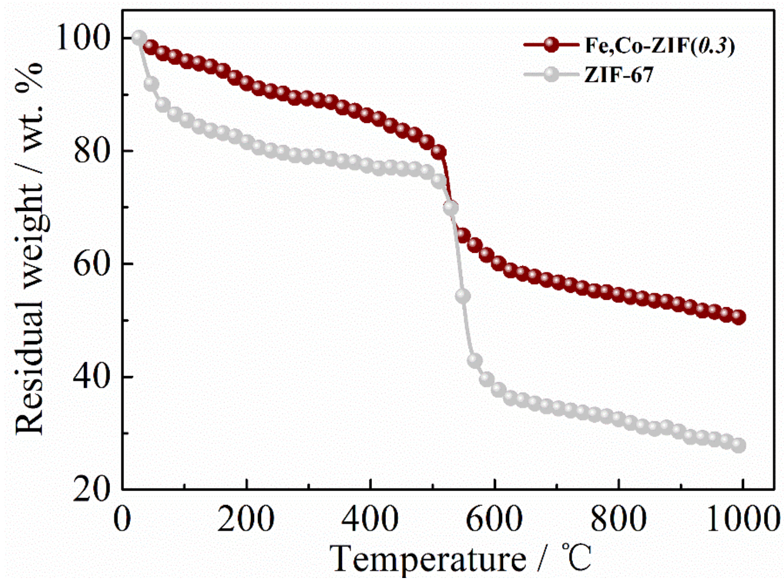

Fig. S3. TG analysis of Fe,Co-ZIF(*0.3*) in comparison with ZIF-67 under Argon atmosphere (temperature ramp rate: 10 ^{o}C min^{-1}).

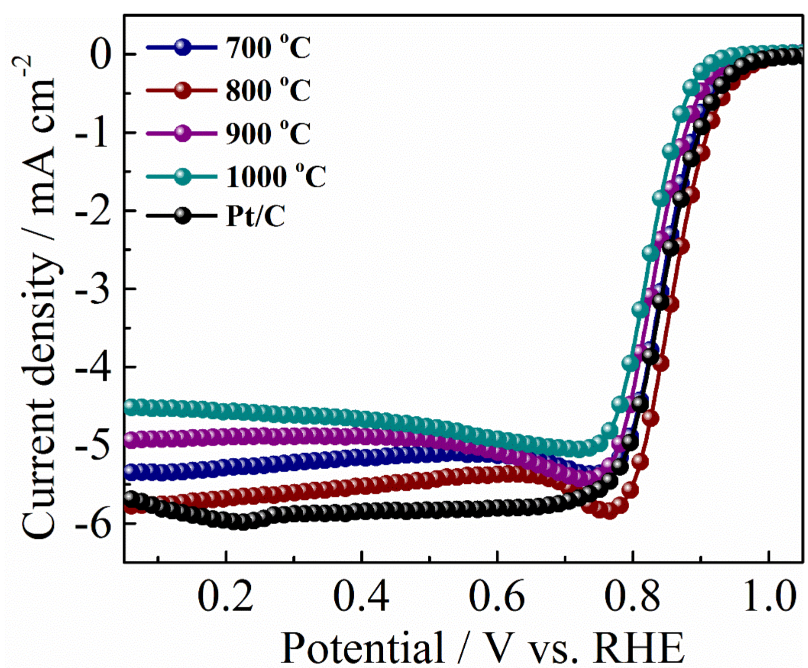

Fig. S4. LSV curves of Fe,Co,N-CNP prepared at various pyrolysis temperatures in O_2-saturated 0.1 M KOH (scan rate: 5 mV s^{-1}, electrode rotation rate: 1600 rpm)

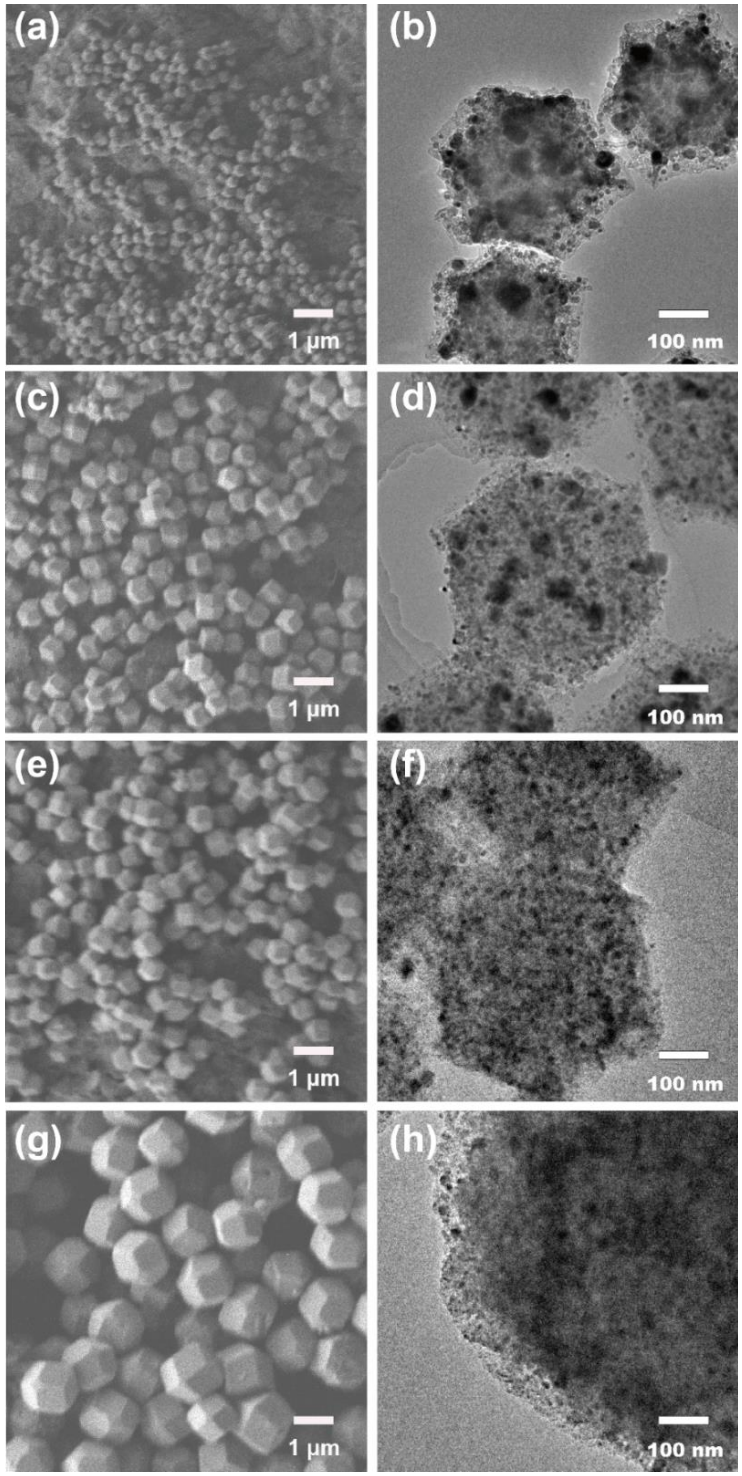

Fig. S5. Representative SEM images of (a) ZIF-67, (c) Fe,Co-ZIF(*0.1*), (e) Fe,Co-ZIF(*0.2*), and (g) Fe,Co-ZIF(*0.3*). HR-TEM images of (b) Co,N-CNP, (d) Fe,Co,N-CNP (*0.1*), (f) Fe,Co,N-CNP (*0.2*), and (h) Fe,Co,N-CNP (*0.3*)

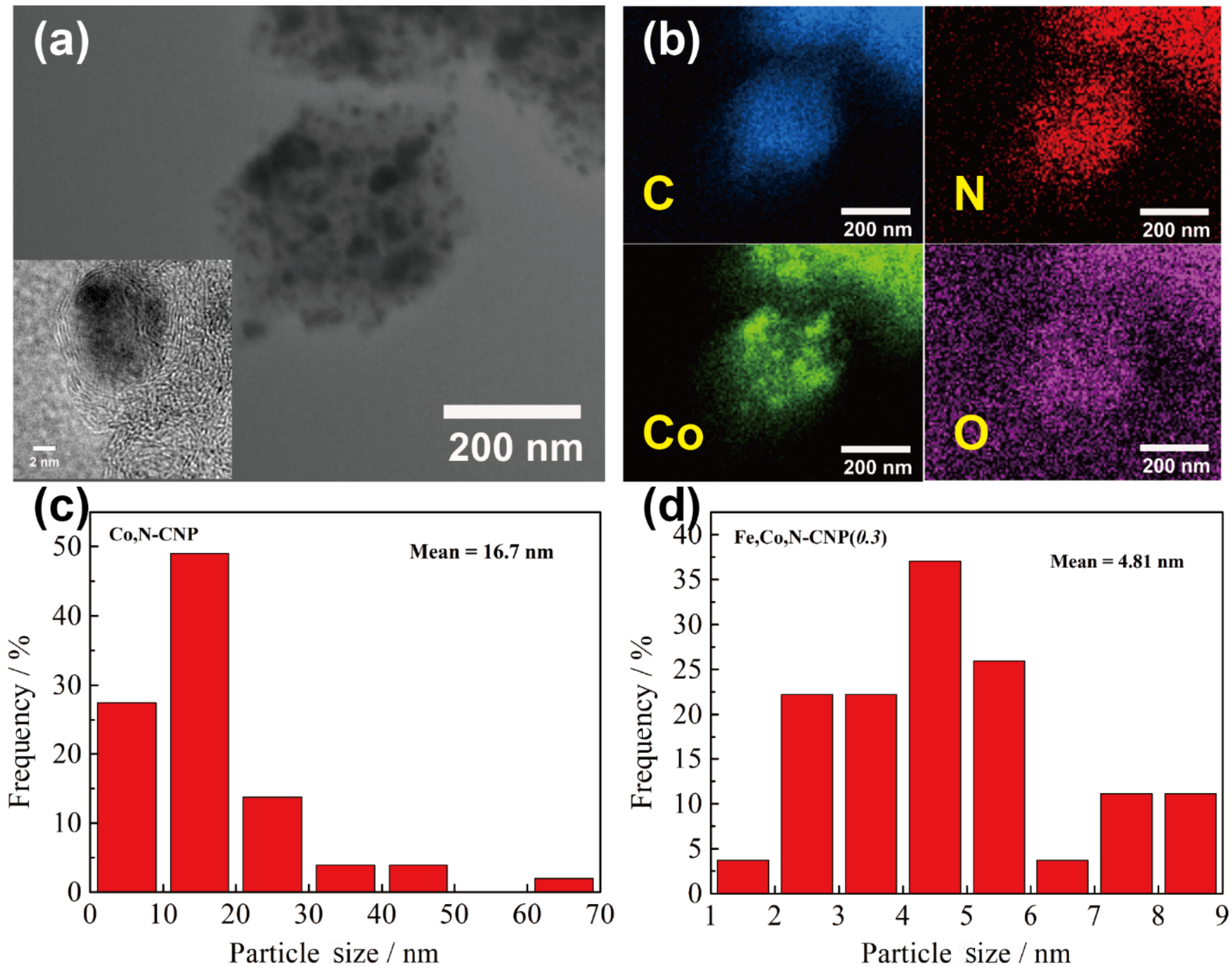

Fig. S6. HR-STEM (a) and the corresponding elemental mapping (b) of Co,N-CNP, and particle distribution of metal NPs in Co,N-CNP (c) and Fe,Co,N-CNP (*0.3*) (d).

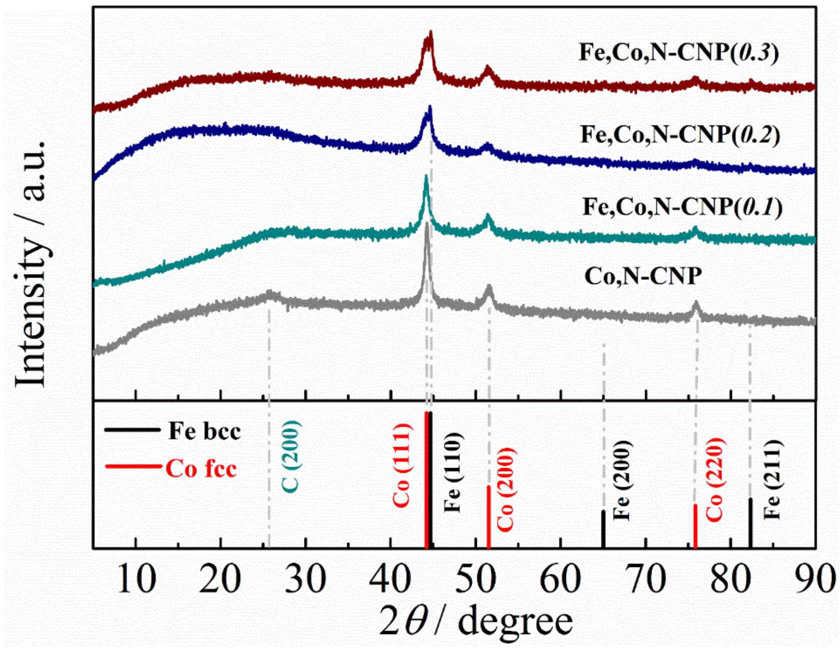

Fig. S7. XRD patterns of Co,N-CNP and Fe,Co,N-CNP(*X*)

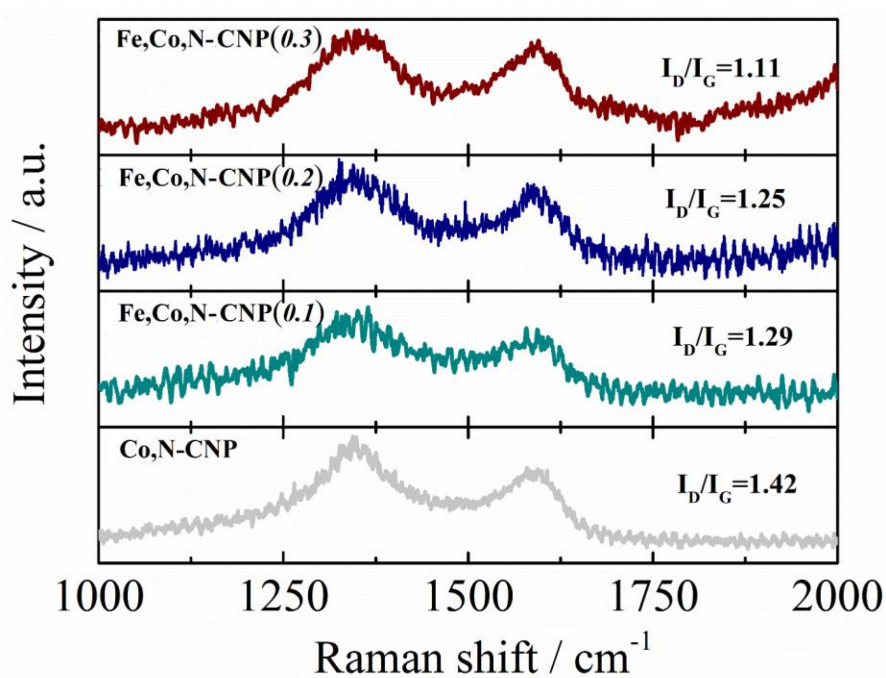

Fig. S8. Raman spectra of Co,N-CNP and Fe,Co,N-CNP(*X*)

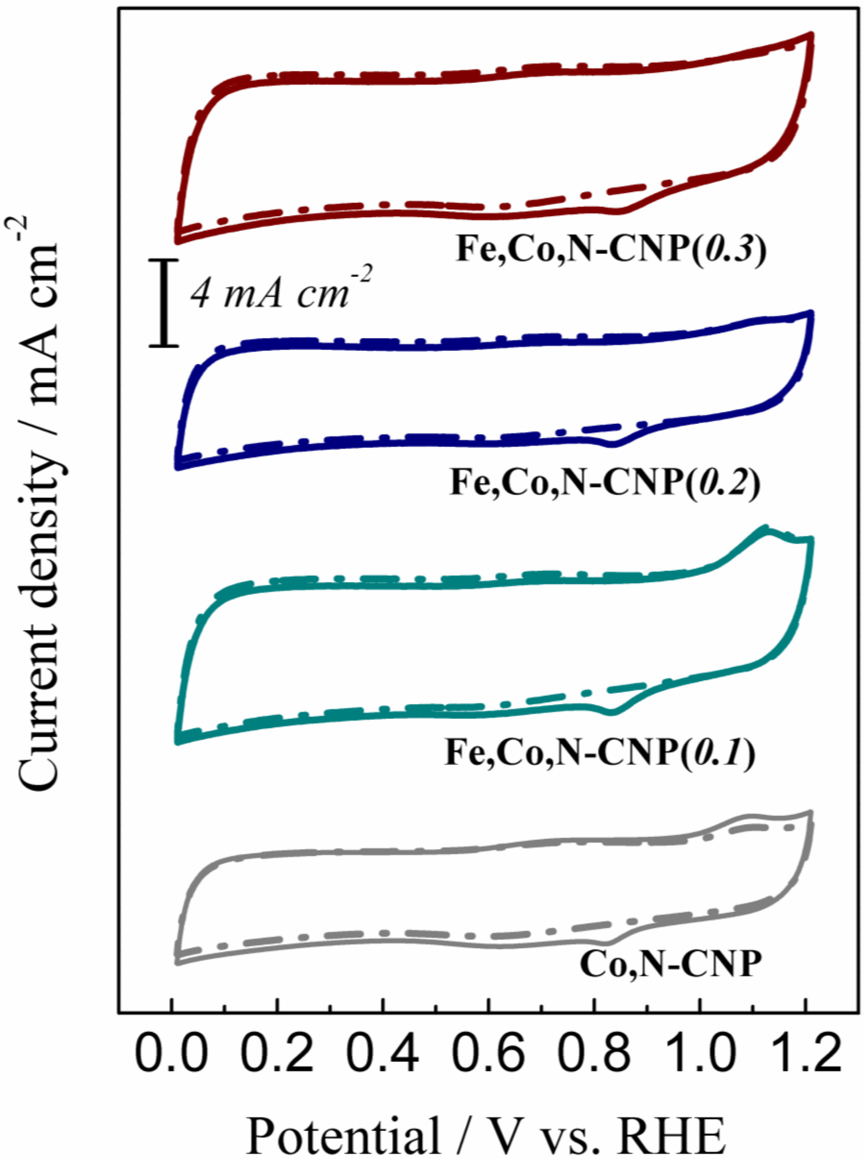

Fig. S9. Comparative CV curves of Co,N-CNP, and Fe,Co,N-CNP(*X*) in N_2- (dotted line) and O_2- (solid line) saturated 0.1 M KOH (scan rate: 50 mV s^{-1}).

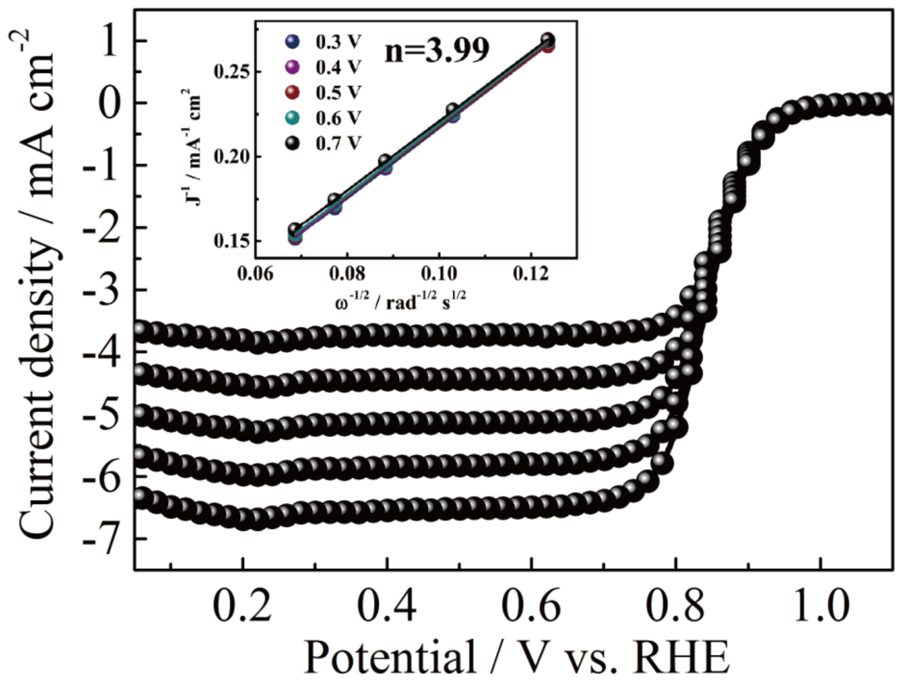

Fig. S10. LSV curves of the commercial Pt/C in O_2-saturated 0.1 M KOH (scan rate: 5 mV s^{-1}) under various rotation rates (Inset: the corresponding K-L plots).

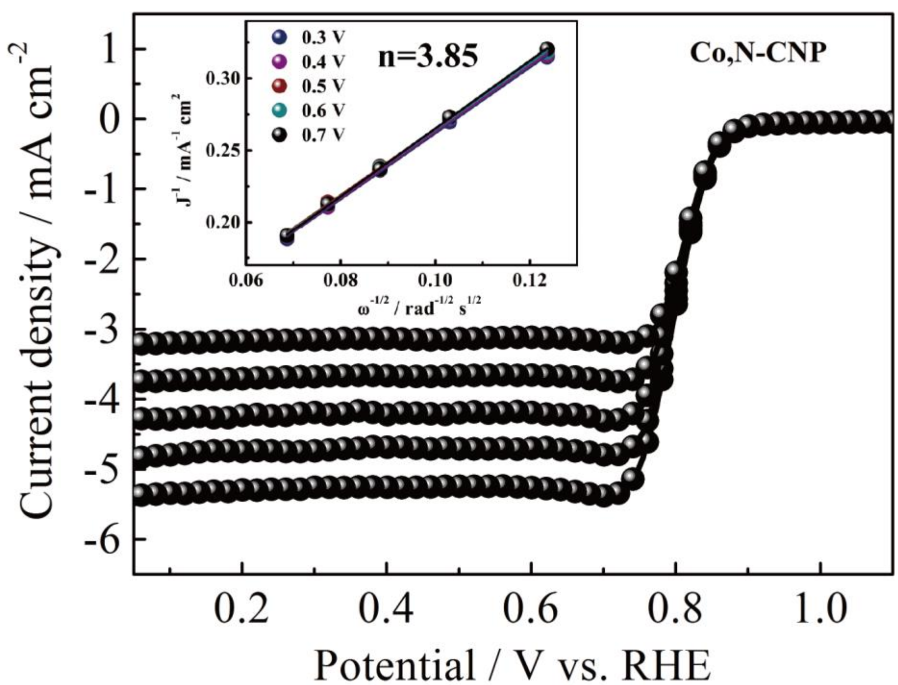

Fig. S11. LSV curves of Co,N-CNP in O_2-saturated 0.1 M KOH (scan rate: 5 mV s^{-1}) under different rotation rates (Inset: the corresponding K-L plots).

Table S1. Pore characteristics of ZIF-67and Fe,Co-ZIF(*X*), and the corresponding electrocatalysts

Sample	S_{BET} ($m^2\ g^{-1}$)	S_{micro} ($m^2\ g^{-1}$)	S_{micro} / S_{BET} (%)	V_{pore} ($cm^3\ g^{-1}$)	Retention rate of S_{mirco}
ZIF-67	1564.4	1515.3	96.7	0.717	-
Co,N-CNP	347.4	153.9	44.3	0.068	10.2
Fe,Co-ZIF(*0.1*)	1456.3	1363.1	93.6	0.758	-
Fe,Co,N-CNP(*0.1*)	413.5	136.3	32.9	0.336	10.0
Fe,Co-ZIF(*0.2*)	1447.4	1353.9	93.5	0.761	-
Fe,Co,N-CNP(*0.2*)	425.3	177.6	41.7	0.349	13.9
Fe,Co-ZIF(*0.3*)	1450.8	1299.5	89.5	0.670	-
Fe,Co,N-CNP(*0.3*)	422.0	204.9	48.6	0.312	15.8

Table S2. N content and configuration determined by XPS in Co,N-CNP and Fe,Co,N-CNP(*X*)

Sample	N (at. %)	Relative content of different N species			
		Pyridinc N	Pyrrolic N	Graphic N	Oxidized N
Co,N-CNP	6.19	51.9	23.0	25.1	0
Fe,Co,N-CNP(*0.1*)	7.45	49.7	29.4	20.9	0
Fe,Co,N-CNP(*0.2*)	8.51	56.8	25.6	17.6	0
Fe,Co,N-CNP(*0.3*)	9.07	48.9	18.9	17.5	14.7

Table S3. The ORR activity of Co,N-CNP and Fe,Co,N-CNP(*X*) in 0.1 M KOH

Sample	$E_{1/2}$ (V)	E_{onset} (V)	J_d / 0.3 V (mA cm^{-2})	J_k / 0.85 V (mA cm^{-2})
Co,N-CNP	0.825	0.893	4.742	1.620
Fe,Co,N-CNP(*0.1*)	0.859	0.957	5.367	7.160
Fe,Co,N-CNP(*0.2*)	0.864	0.953	5.610	9.280
Fe,Co,N-CNP(*0.3*)	0.875	0.979	5.355	12.55
Pt/C	0.846	0.941	5.890	5.150

Table S4. Summary of ORR acitiviy of the non-precious electrocatalysts in 0.1 M KOH electrolyte reported in literatures

Sample	E_{onset} (V vs. RHE)	$E_{1/2}$ (V vs. RHE)	Ref.
NGPC/NCNT	0.94	0.82	S1
hybrid FeNC-20-1000	1.040	0.880	S2
Co-N-C	~0.982	0.871	S3
C_3N_4@NH_2-MIL-101- 700	0.990	0.840	S4
Au@Zn−Fe−C	0.940	N/A	S5
MOFs-800	0.90	0.80	S6
CNPs	1.03	0.92	S7
FeNi@NC_X	1.03	0.86	S8
FePc/MWCNTs	0.916	N/A	S9
DCI-Fe-700	N/A	0.839	S10
CPM-99Fe/C	0.950	0.802	S11
Fe,Co,N-CNP(*0.3*)	0.979	0.875	This work

Table S5. The ORR activity of Co,N-CNP and Fe,Co,N-CNP(*X*) in 0.1 M $HClO_4$

Sample	$E_{1/2}$ (V)	E_{onset} (V)	J_d / 0.3 V (mA cm^{-2})	J_k / 0.75 V (mA cm^{-2})
Co,N-CNP	0.671	0.780	4.969	0.539
Fe,Co,N-CNP(*0.1*)	0.734	0.824	6.081	1.674
Fe,Co,N-CNP(*0.2*)	0.756	0.867	5.636	1.970
Fe,Co,N-CNP(*0.3*)	0.764	0.871	5.788	2.163
Pt/C	0.814	0.901	5.926	2.860

Table S6. Summary of ORR activity of the non-precious electrocatalsyts in 0.1 M $HClO_4$ electrolyte reported in literatures

Sample	E_{onset} (V vs. RHE)	$E_{1/2}$ (V vs. RHE)	Ref.
C-Fe-Z8-Ar	0.95	0.82	S12
ZIF-67	0.86	0.71	S13
meso/micro-PoPD	0.84	~0.70	S14
hybrid FeNC-20-1000	0.9	0.770	S2
Co-N-C	N/A	0.761	S3
S−Fe/N/C	N/A	0.825	S15
$Zn(Im)_2$	0.881	0.73	S16
CoIm	0.83	0.68	S17
C-Fe-ZIF-900-0.84	N/A	0.77	S18
Fe,Co,N-CNP(*0.3*)	0.871	0.764	This work

References

[S1] Zhang, L.; Wang, X.; Wang, R.; Hong, M. Structural Evolution from Metal–Organic Framework to Hybrids of Nitrogen-Doped Porous Carbon and Carbon Nanotubes for Enhanced Oxygen Reduction Activity. *Chem. Mater.* **2015**, *27*, 165-179.

[S2] Liu, T.; Zhao, P.; Hua, X.; Luo, W.; Chen, S.; Cheng, G. An Fe–N–C Hybrid Electrocatalyst derived from a Bimetal–Organic Framework for Efficient Oxygen Reduction. *J. Mater. Chem. A* **2016**, *4*, 11357-11364.

[S3] You, B.; Jiang, N.; Sheng, M.; Drisdell, W. S.; Yano, J.; Sun, Y. Bimetal–Organic Framework Self-Adjusted Synthesis of Support-Free Nonprecious Electrocatalysts for Efficient Oxygen Reduction. *ACS Catal.* **2015**, *5*, 7068-7076.

[S4] Gu, W.; Hu, L.; Li, J.; Wang, E. Hybrid of g-C_3N_4 Assisted Metal-Organic Frameworks and Their Derived High-Efficiency Oxygen Reduction Electrocatalyst in the Whole pH Range. *ACS Appl. Mater. & Inter.* **2016**, *8*, 35281-35288.

[S5] Lu, J.; Zhou, W.; Wang, L.; Jia, J.; Ke, Y.; Yang, L.; Zhou, K.; Liu, X.; Tang, Z.; Li, L. Core–Shell Nanocomposites Based on Gold Nanoparticle@Zinc–Iron-Embedded Porous Carbons Derived from Metal–Organic Frameworks as Efficient Dual Catalysts for Oxygen Reduction and Hydrogen Evolution Reactions. *ACS Catal.* **2016**, *6*, 1045-1053.

[S6] Zhong, H.; Luo, Y.; He, S.; Tang, P.; Li, D.; Alonsovante, N.; Feng, Y. Electrocatalytic Cobalt Nanoparticles Interacting with Nitrogen-Doped Carbon Nanotube in Situ Generated from a Metal–Organic Framework for the Oxygen Reduction Reaction. *ACS Appl. Mater. & Inter.* **2017**, *9*, 2541-2549.

[S7] Zhao, S.; Yin, H.; Du, L.; He, L.; Zhao, K.; Chang, L.; Yin, G.; Zhao, H.; Liu, S.; Tang, Z. Carbonized Nanoscale Metal-Organic Frameworks as High Performance Electrocatalyst for

Oxygen Reduction Reaction. *ACS Nano* **2014**, *8*, 12660-12668.

[S8] Zhu, J.; Xiao, M.; Zhang, Y.; Jin, Z.; Peng, Z.; Liu, C.; Chen, S.; Ge, J.; Xing, W. Metal–Organic Framework-Induced Synthesis of Ultrasmall Encased NiFe Nanoparticles Coupling with Graphene as an Efficient Oxygen Electrode for a Rechargeable Zn–Air Battery. *ACS Catal.* **2016**, *6*, 6335-6342.

[S9] Jahan, M.; Bao, Q.; Loh, K. P. Electrocatalytically Active Graphene–Porphyrin MOF Composite for Oxygen Reduction Reaction. *J. Am. Chem. Soc.* **2012**, *134*, 6707-6713.

[S10] Li, Z.; Sun, H.; Wei, L.; Jiang, W. J.; Wu, M.; Hu, J. S. Lamellar Metal Organic Framework Derived Fe-N-C Non-noble Electrocatalysts with Bimodal Porosity for Efficient Oxygen Reduction. *ACS Appl. Mater. & Inter.* **2017**, *9*, 5272-5278.

[S11] Lin, Q.; Bu, X.; Kong, A.; Mao, C.; Zhao, X.; Bu, F.; Feng, P. New Heterometallic Zirconium Metalloporphyrin Frameworks and their Heteroatom-Activated High-Surface-Area Carbon Derivatives. *J. Am. Chem. Soc.* **2015**, *137*, 2235-2238.

[S12] Wang, X.; Zhang, H.; Lin, H.; Gupta, S.; Wang, C.; Tao, Z.; Fu, H.; Wang, T.; Zheng, J.; Wu, G. Directly Converting Fe-Doped Metal–Organic Frameworks into Highly Active and Stable Fe-N-C Catalysts for Oxygen Reduction in Acid. *Nano Energy* **2016**, *25*, 110-119.

[S13] Xia, W.; Zhu, J.; Guo, W.; An, L.; Xia, D.; Zou, R. Well-Defined Carbon Polyhedrons Prepared from Nano Metal-Organic Frameworks for Oxygen Reduction. *J. Mater. Chem. A* **2014**, *2*, 11606-11613.

[S14] Liang, H. W.; Zhuang, X.; Brüller, S.; Feng, X.; Müllen, K. Hierarchically Porous Carbons with Optimized Nitrogen Doping as Highly Active Electrocatalysts for Oxygen Reduction. *Nat. Commun.* **2014**, *5*, 4973.

[S15] Hu, K.; Tao, L.; Liu, D.; Huo, J.; Wang, S. Sulfur-Doped Fe/N/C Nanosheets as Highly-

Efficient Electrocatalysts for Oxygen Reduction Reaction. *ACS Appl. Mater. & Inter.* **2016**, *8*, 19379-19385.

[S16] Zhao, D.; Shui, J. L.; Grabstanowicz, L. R.; Chen, C.; Commet, S. M.; Xu, T.; Lu, J.; Liu, D. J. Highly Efficient Non-Precious Metal Electrocatalysts Prepared from One-Pot Synthesized Zeolitic Imidazolate Frameworks. *Adv. Mater.* **2014**, *26*, 1093-1097.

[S17] Ma, S.; Goenaga, G. A.; Call, A. V.; Liu, D. J. Cobalt Imidazolate Framework as Precursor for Oxygen Reduction Reaction Electrocatalysts. *Chemistry* **2011**, *17*, 2063-2067.

[S18] Deng, Y.; Dong, Y.; Wang, G.; Sun, K.; Shi, X.; Zheng, L.; Li, X.; Liao, S. Well-Defined ZIF-Derived Fe-N Codoped Carbon Nanoframes as Efficient Oxygen Reduction Catalysts. *ACS Appl. Mater. & Inter.* **2017**, *9*, 9699-9709.